American Mineralogist, Volume 109, pages 624–627, 2024

Letter

A simple method for obtaining heat capacity coefficients of minerals

Samuel Bowman[1,*], Arkajyoti Pathak[1], Vikas Agrawal[1], and Shikha Sharma[1]

[1]Department of Geology and Geography, West Virginia University, Morgantown, West Virginia 26506, U.S.A.

Abstract

Heat capacity data are unavailable or incomplete for many minerals at geologically relevant temperatures. Despite the availability of entropy and enthalpy values in numerous thermodynamic tables (even sometimes at elevated temperatures), there remains need for extrapolation beyond, or interpolation between, temperatures. This approach inevitably results in estimates for entropy and enthalpy values because the heat capacity coefficients required for optimal thermodynamic treatment are less frequently available. Here we propose a simple method for obtaining heat capacity coefficients of minerals. This method requires only the empirically measured temperature-specific heat capacity for calculation via a matrix algorithm. The system of equations solver is written in the Python computing language and has been made accessible in an online repository. Thermodynamically, the solution to a system of equations represents the heat capacity coefficients that satisfy the mineral-specific polynomial. Direct coefficient calculation will result in more robust thermodynamic data, which are not subject to fitting uncertainties. Using hematite as an example, this method provides results that are comparable to conventional means and is applicable to any solid material. Coefficients vary within the traditional large 950 K temperature interval, indicating that best results should instead utilize a smaller 400 K temperature interval. Examples of large-scale implications include the refinement of geothermal gradient estimation in rapidly subsiding sedimentary basins or metamorphic and hydrothermal evolution.

Keywords: Gaussian elimination, heat capacity, hematite, system of equations

Introduction

Earth systems are rarely, if ever, truly at standard temperature and pressure; the effect of these parameters must be considered for robust thermodynamic treatment. Regarding systems at non-standard temperatures, mineralogists and petrologists employ (directly or indirectly) the heat capacity (C_P) for the selected material(s) for purposes such as studying the effects of temperature and pressure for basin modeling or maturity modeling (Waples and Waples 2004). However, despite the wide availability of C_P data for many minerals, in most cases the numbers are often applicable to narrow temperature ranges. In other cases, the entropy (ΔS) and enthalpy (ΔH) must either be extrapolated or interpolated to the desired temperature (Robie and Hemingway 1995), or the final free energy (ΔG_f) is obtained via linear regression (Toulmin and Barton 1964). Considering that C_P follows a polynomial trend for temperature, it is expected that linear regressions of free energy may introduce uncertainty (although linear behavior may provide reasonable estimates for free energy using small ΔT intervals). One limitation within the present heat capacity literature may be found for the mineral hematite in Hemingway (1990), where there is a function discontinuity occurring at 950 K between the lower (T <950 K) and upper (T >950 K) temperature domains. The heat capacity of a solid is typically continuous except for occasional discontinuities and has been attributed to crystallographic/phase transitions (e.g., Guyot et al. 1993). Heat capacity function discontinuities will be translated to the calculated or regressed polynomial coefficients. Ideally, the characteristic mineral specific C_P coefficients have been determined and published, allowing for exact calculation of entropy and enthalpy at a given temperature. Unfortunately, these coefficients are often unavailable throughout the literature, one notable exception being the compilation in Robie and Hemingway (1995).

Fundamentally, the heat capacity of a material is effectively the input energy required to raise the thermal energy of that same material. The heat capacity is vital to mineralogical, petrological, and geochemical research. It is quantified for a selected material using various calorimetric techniques and when plotted against temperature, takes the form of a polynomial (e.g., Klemme and van Miltenburg 2003; Benisek et al. 2012). The C_P polynomial order and the number of coefficients varies throughout the literature. For example, the form in Xiong et al. (2016) contains seven coefficients and is a third-order polynomial, while the Shomate equation (e.g., NIST) has five coefficients and is also a third-order polynomial, while the progenitor, the Maier-Kelley form contains only three coefficients and is a second-order polynomial (Maier and Kelley 1932). The form commonly found associated with geological solids or minerals is the second-order polynomial with five coefficients, as given by Hemingway et al. (1978). Finally, the C_P polynomial formula is often determined by regression of existing data to fit a specific polynomial form (Hemingway 1990; Waples and Waples 2004). The primary goal of this study is to evaluate the polynomial through direct means. This

* E-mail: sabowman@mix.wvu.edu. Orcid 0000-0002-1510-174X

0003-004X/24/0003–624$05.00/DOI: https://doi.org/10.2138/am-2023-9109

approach allows for smaller ΔT to be utilized and eliminates any introduced fitting bias (e.g., overfitting; see Gamsjäger and Wiessner 2018). Therefore, employing this direct coefficient calculation technique relies solely upon the empirical C_P, ensuring that the polynomial retains fidelity. In other words, as the direct calculation is axiomatically correct, the values obtained from the equation proposed in this contribution will remove much of the errors associated with measurements from interpolated and extrapolated values available in the literature so far. Finally, this method can be used to directly calculate thermal diffusivity, a crucial physical parameter of geological systems that reflects the ability to conduct thermal energy relative to its ability to store the energy (Fuchs et al. 2021). Applications of accurate heat capacity measurement are in the fields of geothermal gradient determination in active basins, basin modeling, and studying geodynamic transformations in tectonically active regions.

Methodology

Theoretical background

Here, we offer a simple method for the determination of the characteristic coefficients requiring only a suite of five C_P values at their corresponding temperatures. For solids, the relationship between heat capacity and temperature is nonlinear (e.g., Robie et al. 1978; Klemme and van Miltenburg 2003; Benisek et al. 2012; Xiong et al. 2016; Ulian et al. 2020; Vassiliev and Taldrik 2021), implying that linear determination of ΔG_f is likely to induce uncertainty of over(under)estimation compared to a polynomial fit. For a C_P equation with five coefficients, there are five vectors, each at five unique temperatures with accompanying scalars. Note that the scalars are equal to the coefficients, which, of course, are the same for all vectors (i.e., all temperatures). The intersection of the vectors is the solution to the system of equations, where there are an equal number of scalar coefficients that satisfy all C_P equations at each temperature simultaneously. Once the scalar coefficients have been evaluated, ΔS, ΔH, and ultimately ΔG_f at a selected temperature may be determined.

For a C_P polynomial with n equations and n coefficients, there is a square n × n matrix, written in the general form **Ax** = **b**, or

$$\begin{bmatrix} a_{11} & \cdots & a_{1n} \\ \vdots & \ddots & \vdots \\ a_{n1} & \cdots & a_{nn} \end{bmatrix} * \begin{bmatrix} x \\ \vdots \\ x_n \end{bmatrix} \quad (1)$$

This method may be employed for any solid substance in which existing C_P data are known at a corresponding temperature. As an illustrative example calculation, let us consider an example of hematite using C_P polynomial found in Hemingway (1990), where

$$C_P = A - BT + CT^2 - DT^{-0.5} + ET^{-2} \quad (2)$$

This form has five coefficients and is a second-order polynomial. Now, for an n × n matrix, there are five reported C_P at five temperatures requiring five equations. Combining the C_P polynomial with Equation 1, **Ax** = **b** becomes (approximately)

$$\begin{bmatrix} 1 & 400 & 1.6E+5 & 0.050 & 8.25E-6 \\ 1 & 500 & 2.5E+5 & 0.045 & 4.00E-6 \\ 1 & 600 & 3.6E+5 & 0.041 & 2.78E-6 \\ 1 & 700 & 4.9E+5 & 0.038 & 2.04E-6 \\ 1 & 800 & 6.4E+5 & 0.035 & 1.56E-6 \end{bmatrix} * \begin{bmatrix} x_1 \\ x_2 \\ x_3 \\ x_4 \\ x_5 \end{bmatrix} = \begin{bmatrix} 120.91 \\ 131.39 \\ 139.01 \\ 146.53 \\ 156.06 \end{bmatrix} \quad (3)$$

Note that **b** to the right of the equals sign in Equation 3 contains the temperature-specific C_P in Hemingway (1990) from 400 to 800 K. The coefficients are obtained through Gaussian elimination and by taking the augmented matrix to reduced row echelon form (rref) via elementary row operations. Rewriting, we find the augmented matrix becomes **A**|**b**

$$\left[\begin{array}{ccccc|c} 1 & 400 & 1.6E+5 & 0.050 & 8.25E-6 & 120.91 \\ 1 & 500 & 2.5E+5 & 0.045 & 4.00E-6 & 131.39 \\ 1 & 600 & 3.6E+5 & 0.041 & 2.78E-6 & 139.01 \\ 1 & 700 & 4.9E+5 & 0.038 & 2.04E-6 & 146.53 \\ 1 & 800 & 6.4E+5 & 0.035 & 1.56E-6 & 156.06 \end{array}\right] \xrightarrow{rref} \left[\begin{array}{ccccc|c} 1 & 0 & 0 & 0 & 0 & 994.40 \\ 0 & 1 & 0 & 0 & 0 & -0.78862 \\ 0 & 0 & 1 & 0 & 0 & 3.9574E-4 \\ 0 & 0 & 0 & 1 & 0 & -1.3361E+4 \\ 0 & 0 & 0 & 0 & 1 & 7.4669E+6 \end{array}\right] \quad (4)$$

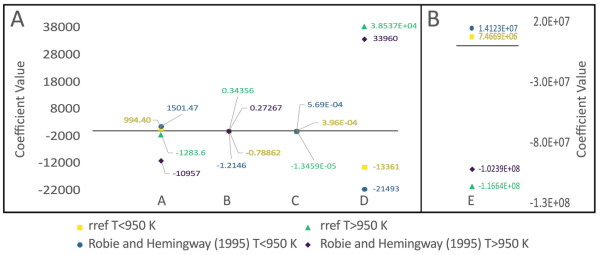

Figure 1. Hematite C_P coefficients across the two major temperature domains as found in Hemingway (1990). The low-temperature domain represents the coefficients for T <950 K, while the high-temperature domain represents the coefficients for T >950 K. Coefficients calculated through rref methodology (400 to 800 K for T <950 K and 1000 to 1400 K for T >950 K) correspond to subintervals 2 and 6 in Table 1, respectively) are compared to those reported in Robie and Hemingway (1995). (**a**) Coefficients A, B, C, and D. (**b**) Coefficient E. (Color online.)

The five coefficients, after the x_n scalar matrix transpose and substitution become

$$\begin{bmatrix} x_1 \\ x_2 \\ x_3 \\ x_4 \\ x_5 \end{bmatrix}^T = \begin{bmatrix} A & B & C & D & E \end{bmatrix} = \begin{bmatrix} 994.40 & -0.78862 & 3.9574E-4 & -1.3361E+4 & 7.4669E+6 \end{bmatrix} \quad (5)$$

where $A = x_1$ and $E = x_5$. Upon coefficient back-substitution into the C_P polynomial, the empirical C_P is returned at each temperature sub-equation. One limitation of this approach is that it requires a square n × n matrix, and thus, the number of temperature sub-equations is limited to the number of coefficients in the polynomial. If there are more temperatures (rows) than coefficients (columns), then A cannot be taken to rref, and the system does not have a solution. It is worth noting that the accuracy and uncertainty of this method it is, of course, limited to the quality of the reported C_P input data.

Software implementation

Manually solving a system of equations by rref is a lengthy process, particularly for non-integer numbers. To this end, it is advantageous to employ a calculator (e.g., online, computer code, etc.). We have developed the C_P Coefficent Calculator (C^3) to calculate the coefficients using the rref method above. Modifying Python3 code found in Kong et al. (2021), C^3 is offered under the MIT license and is available (along with a README manual) at https://github.com/WVUStableIsotopeLab/CodeswithPython.

Results and discussion

As an example, hematite C_P coefficients obtained from rref calculation are provided in Table 1 (subinterval 2) and are presented in Figure 1. These data are computed across two major temperature domains (298.15 to 950 K and 950 to 1800 K) (Hemingway 1990). Given the sensitivity of the coefficients, the rref direct-calculated results compare favorably to the hematite values reported by Robie and Hemingway (1995). For the upper-temperature interval (950 to 1800 K), our proposed method yields an additional coefficient that is not available, as noted in the existing literature. Robie and Hemingway (1995) provide a line of best-fit regression coefficients over the range of 298 to 1800 K for A, B, and C of –808.9, 0.2466, and –8.423E-5, respectively. This is compared to the direct calculation method presented here, where five coefficients are calculated over a much more condensed temperature range from 400 to 800 K in 100 K increments. We believe that our approach is likely to be

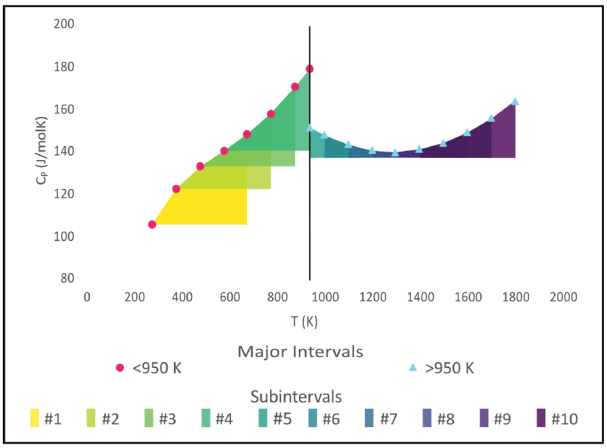

Figure 2. Hematite heat capacity values, as reported in Hemingway (1990), with corresponding temperature intervals (as given in Table 1). The numbered temperature subintervals are those that were used to evaluate the polynomial coefficients reported in Table 1 at each interval. Red dots and blue triangles are the respective <950 K and >950 K of the major "two-domain" temperature intervals. Black line indicates function discontinuity at 950 K. (Color online.)

more accurate as the temperature interval is significantly reduced and does not cross any phase transition (e.g., 950 K in Fig. 2). In addition, because the relationship between temperature and C_P is nonlinear, the curve-fitting approach is particularly susceptible to extrapolation since the rate of change is not constant (i.e., $d^2y/dx^2 \neq 0$). Regarding interpolation, empirical $C_P(T)$ data used in both curve-fitting and direct calculation may be improved by reducing the temperature interval between interpolations. These temperature intervals are often given in 100 K increments (e.g., Robie and Hemingway 1995). It is worth mentioning that the direct calculation method is an interpolative approach and, thus, is subject to the quality of the $C_P(T)$ data and the temperature increments. If, for example, the temperature increment was decreased to 50 K, the resulting $C_P(T)$ would likely lead to even more accurate coefficients. In this scenario, five coefficients could still be determined but over a tighter temperature interval (400, 450, 500, 550, and 600 K).

One of the most striking observations of the tabulated data is that it may display discontinuous behavior when plotted graphically, particularly at the interface between the low- and high-temperature domain intervals (~950 K) (Fig. 2). Moreover, note the change in the concavity between the low- and high-temperature domain intervals. The highest C_P value across the entire temperature range is at 950 K, and the significant trough is about ~1300 K. This observation, along with the discontinuity at 950 K, indicate that the resulting coefficients will be subsequently affected. Indeed, when temperature intervals of ~400 K are utilized, the coefficients are not static but drift (Table 1). It is apparent that the most accurate coefficients are those which minimize temperature drift obtained by performing the rref calculation over a small ΔT interval. Since entropy and enthalpy are produced from integrating C_P°/T and C_P (where C_P is the selected polynomial with commensurate coefficients) over a range starting at 298.15 K, it is reasonable to use, say for a temperature of 780 K, coefficients that pertain to a subinterval (i.e., subintervals 2 or 3 in Fig. 2 and Table 1) instead of conventional coefficients for the entire 298.15 to 950 K domain. For the temperature intervals <950 K, the behavior is relatively linear (subintervals 1 to 4 in Fig. 2). In comparison, the temperature intervals >950 K are parabolic about the local minimum at ~1300 K. This behavior is translated to the C_P values as well (subinterval 6 in Fig. 2 and Table 1).

Implications

The heat capacity is a fundamental aspect not only limited to minerals but also liquids, gases, and dissolved species. It underlies thermodynamics as it is necessary for entropy, enthalpy, and, ultimately, free energy calculations. The direct calculation method provided above requires only empirical C_P for data input, thus avoiding curve-fitting uncertainties or human-induced bias. Therefore, the utility of this method is vast and has direct application to fluid-rock interactions. Specific examples including slab-subduction (i.e., Peacock 1987), hydrothermal or geothermal systems, and equilibrium speciation modeling. While the mineral hematite was used as an illustrative example, this method has been applied to diamond due to its use in high-temperature mantle research (e.g., Stachel et al. 2022) and to quartz because of its ubiquity. In addition, we have applied this method to mineral assemblages used in geothermometry, including galena-pyrite-sphalerite (Smith et al. 1977), biotite-garnet (as pyrope and almandine) (Ferry and Spear 1978), and muscovite-biotite (e.g., Hoisch 1989). The C_P coefficients for almandine, diamond, muscovite, pyrite, pyrope, quartz, and sphalerite have been calculated over at least two temperature domains and are compared against tabulated values. These results are provided as Online Materials[1]. The method given above, however, can still be improved. Future work could examine coefficient behavior

Table 1. Heat capacity coefficients for hematite calculated at ΔT of ~400 K using rref and $C_P(T)$ found in Hemingway (1990)

T Interval (K-K)	Fig. 2 Interval no.	Hematite heat capacity coefficients				
		A	*B*	*C*	*D*	*E*
298.15–700	1	841.57	−0.65736	3.3946E-04	−1.0901E+04	5.2795E+06
400–800	2	994.40	−0.78862	3.9574E-04	−1.3361E+04	7.4669E+06
500–900	3	1.1801E+03	−0.92370	4.4462E-04	−1.6606E+04	1.1139E+07
600–950	4	1.3253E+03	−1.0102	4.7053E-04	−1.9417E+04	1.5526E+07
950–1300	5	−402.36	−9.0874E-03	5.7717E-05	1.7680E+04	−5.6871E+07
1000–1400	6	−1283.6	0.34356	−1.3459E-05	3.8537E+04	−1.1664E+08
1100–1500	7	−579.09	−0.10303	2.8004E-05	2.0480E+04	−5.0923E+07
1200–1600	8	−448.63	5.9654E-02	3.5304E-05	1.7089E+04	3.7975E+07
1300–1700	9	2.9410E+03	−0.92811	1.8031E-04	−7.6875E+04	3.9375E+08
1400–1800	10	88.544	−5.8354E-02	4.6708E-05	416.67	6.2500E+07

by dividing temperature domains into smaller ΔT subsections. Generation of C_P coefficients from rref direct calculation for smaller temperature intervals is expected to be more accurate than using coefficients under the conventional "two-domain" approach—especially for temperatures where discontinuities occur (e.g., ~900 to 1300 K for hematite in Intervals 5 and 6 in Table 1 and Fig. 2). Finally, developing an understanding of the interesting local minimum at ~1300 K would almost certainly prove fruitful.

Acknowledgments and Funding

The authors thank S. Bhattacharya for proofreading and providing helpful comments on this manuscript. The authors also acknowledge the Department of Energy Office of Energy Efficiency & Renewable Energy (DOE EERE) Geothermal Technologies Program Award DE-EE0009597 to S. Sharma.

References cited

Benisek, A., Kroll, H., and Dachs, E. (2012) The heat capacity of fayalite at high temperatures. American Mineralogist, 97, 657–660, https://doi.org/10.2138/am.2012.3924.

Ferry, J.M. and Spear, F.S. (1978) Experimental calibration of the partitioning of Fe and Mg between biotite and garnet. Contributions to Mineralogy and Petrology, 66, 113–117, https://doi.org/10.1007/BF00372150.

Fuchs, S., Förster, H.J., Norden, B., Balling, N., Miele, R., Heckenbach, E. and Förster, A. (2021) The thermal diffusivity of sedimentary rocks: Empirical validation of a physically based $\alpha - \varphi$ relation. Journal of Geophysical Research: Solid Earth, 126, e2020JB020595.

Gamsjäger, E. and Wiessner, M. (2018) Low temperature heat capacities and thermodynamic functions described by Debye-Einstein integrals. Monatshefte für Chemie—Chemical Monthly, 149, 357–368.

Guyot, F., Richet, P., Courtial, P., and Gillet, P. (1993) High-temperature heat capacity and phase transitions of $CaTiO_3$ perovskite. Physics and Chemistry of Minerals, 20, 141–146, https://doi.org/10.1007/BF00200116.

Hemingway, B.S. (1990) Thermodynamic properties for bunsenite, NiO, magnetite, Fe_3O_4, and hematite, Fe_2O_3, with comments on selected oxygen buffer reactions. American Mineralogist, 75, 781–790.

Hemingway, B.S., Robie, R.A., and Kittrick, J.A. (1978) Revised values for the Gibbs free energy of formation of $[Al(OH)_{4\,aq}^-]$, diaspore, boehmite and bayerite at 298.15 K and 1 bar, the thermodynamic properties of kaolinite to 800 K and 1 bar, and the heats of solution of several gibbsite samples. Geochimica et Cosmochimica Acta, 42, 1533–1543, https://doi.org/10.1016/0016-7037(78)90024-8.

Hoisch, T.D. (1989) A muscovite-biotite geothermometer. American Mineralogist, 74, 565–572.

Klemme, S. and van Miltenburg, J.C. (2003) Thermodynamic properties of hercynite ($FeAl_2O_4$) based on adiabatic calorimetry at low temperatures. American Mineralogist, 88, 68–72, https://doi.org/10.2138/am-2003-0108.

Kong, Q., Siauw, T., and Bayen, A.M. (2021) Python Programming and Numerical Methods: A Guide for Engineers and Scientists, 456. Academic Press.

Maier, C.G. and Kelley, K.K. (1932) An equation for the representation of high-temperature heat content data. Journal of the American Chemical Society, 54, 3243–3246, https://doi.org/10.1021/ja01347a029.

Peacock, S.M. (1987) Thermal effects of metamorphic fluids in subduction zones. Geology, 15, 1057–1060, https://doi.org/10.1130/0091-7613(1987)15<1057:TEOMFI>2.0.CO;2.

Robie, R.A. and Hemingway, B.S. (1995) Thermodynamic properties of minerals and related substances at 298.15 K and 1 Bar (10^5 Pascals) pressure and at higher temperatures. U.S. Geological Survey Bulletin, 2131, 461. U.S. Department of the Interior.

Robie, R.A., Hemingway, B.S., and Wilson, W.H. (1978) Low-temperature heat capacities and entropies of feldspar glasses and of anorthite. American Mineralogist, 63, 109–123.

Smith, J.W., Doolan, S., and McFarlane, E.F. (1977) A sulfur isotope geothermometer for the trisulfide system galena-sphalerite-pyrite. Chemical Geology, 19, 83–90, https://doi.org/10.1016/0009-2541(77)90006-7.

Stachel, T., Cartigny, P., Chacko, T., and Pearson, D.G. (2022) Carbon and nitrogen in mantle-derived diamonds. Reviews in Mineralogy and Geochemistry, 88, 809–875, https://doi.org/10.2138/rmg.2022.88.15.

Toulmin, P. III and Barton, P.B. II (1964) A thermodynamic study of pyrite and pyrrhotite. Geochimica et Cosmochimica Acta, 28, 641–671, https://doi.org/10.1016/0016-7037(64)90083-3.

Ulian, G., Moro, D., and Valdré, G. (2020) Thermodynamic and thermoelastic properties of wurtzite-ZnS by density function theory. American Mineralogist, 105, 1212–1222, https://doi.org/10.2138/am-2020-7330.

Vassiliev, V.P. and Taldrik, A.F. (2021) Description of the heat capacity of solid phases by a multiparameter family of functions. Journal of Alloys and Compounds, 872, 159682, https://doi.org/10.1016/j.jallcom.2021.159682.

Waples, D.W. and Waples, J.S. (2004) A review and evaluation of specific heat capacities of rocks, minerals and subsurface fluids. Part 1: Minerals and nonporous rocks. Natural Resources Research, 13, 97–122, https://doi.org/10.1023/B:NARR.0000032647.41046.e7.

Xiong, Z., Liu, X., Shieh, S.R., Wang, S., Chang, L., Tang, J., Hong, X., Zhang, Z., and Wang, H. (2016) Some thermodynamic properties of larnite (β-Ca_2SiO_4) constrained by high T/P experiment and/or theoretical simulation. American Mineralogist, 101, 277–288, https://doi.org/10.2138/am-2016-5425.

Manuscript received June 23, 2023
Manuscript accepted December 4, 2023
Accepted manuscript online December 13, 2023
Manuscript handled by Di Wu

Endnote:

[1]Deposit item AM-24-39109. Online Materials are free to all readers. Go online, via the table of contents or article view, and find the tab or link for supplemental materials.